Journal of Minerals and Materials Characterization and Engineering, 2017, 5, 323-338
http://www.scirp.org/journal/jmmce
ISSN Online: 2327-4085
ISSN Print: 2327-4077

Simulation and Optimization Characteristic of Novel MoS_2/c-Si HIT Solar Cell

Sue Xu[1], Xiangbin Zeng[2*], Wenzhao Wang[2], Guangtong Zhou[1], Yishuo Hu[2], Shaoxiong Wu[2], Yang Zeng[2]

[1]China-EU Institute for Clean and Renewable Energy, Huazhong University of Science & Technology, Wuhan, China
[2]School of Optical and Electronic Information, Huazhong University of Science & Technology, Wuhan, China
Email: *eexbzeng@163.com

How to cite this paper: Xu, S., Zeng, X.B., Wang, W.Z., Zhou, G.T., Hu, Y.S., Wu, S.X. and Zeng, Y. (2017) Simulation and Optimization Characteristic of Novel MoS_2/c-Si HIT Solar Cell. *Journal of Minerals and Materials Characterization and Engineering*, **5**, 323-338.
https://doi.org/10.4236/jmmce.2017.55027

Received: August 11, 2017
Accepted: September 25, 2017
Published: September 28, 2017

Abstract

Monolayer Mos_2 has excellent optoelectronic properties, which is a potential material for solar cell. Though MoS_2/c-Si heterojunction solar cell has been researched by many groups, little study of MoS_2/c-Si solar cell physics is reported. In this paper, MoS_2/c-Si heterojunction solar cells have been designed and optimized by AFORS-HET simulation program. The various factors affecting the performance of the cells were studied in details using TCO/n-type MoS_2/i-layer/p-type c-Si/BSF/Al structure. Due to the important role of intrinsic layer in HIT solar cell, the effect of different intrinsic layers including a-Si:H, nc-Si:H, a-SiGe:H, on the performance of TCO/n-type MoS_2/i-layer/p-type c-Si/Al cell, was studied in this paper. The results show that the TCO/n-type MoS_2/i-layer/p-type c-Si/Al cell has the highest efficiency with a-SiGe:H as intrinsic layer, efficiency up to 21.85%. The back surface field effects on the properties of solar cells were studied with p + μc-Si and Al as BSF layers. And the effect of various factors such as thickness and band gap of intrinsic layer, thickness of MoS_2, density of defect state and the energy band offset of MoS_2/c-Si interface of TCO/n-type MoS_2/i-layer nc-Si:H/p-type c-Si/Al cells, on the characteristics of solar cells, have been discussed for this kind of MoS_2 heterojunction cells. The optimal solar cell with structure of TCO/n-type MoS_2/i-type nc-Si:H/p-type c-Si/BSF/Al, has the best efficiency of 27.22%.

Keywords

Intrinsic Material, Cell Efficiency, Molybdenum Disulfide

1. Introduction

Since physicists Andre Anaheim and Konstantin Novoselov successfully isolated graphene from graphite in 2004 [1], two dimensional layered materials have

been widely concerned due to its excellent physical and chemical properties. However, graphene is a zero-gap material, which limits its applications in some fields. Recently, researchers have been refocusing on other grapheme, like 2D materials to overcome the shortage of graphene and broaden its range of applications. In contrast to the zero-gap graphene, transition metal sulfides are tuneable band structure and applicable in wide fields due to its excellent optional and electrical properties [2] [3]. Monolayer MoS_2 has an ultra-thin lamellar structure with thickness about 0.65 nm [4], a direct band gap of 1.9 eV [5], and high electron mobility of 200 $cm^2 \cdot V^{-1} \cdot s^{-1}$ [6]. So it is a potential candidate material for TFTs, FETs, photodetectors, sensors and solar cells.

It has been reported that MoS_2 exhibits one order of magnitude higher light absorption than Si and GaAs [7]. MoS_2/c-Si heterojunction solar cell has been researched by many groups lately. L. Hao *et al.* achieved a PCE of 1.3% in MoS_2/Si junction by the method of magnetron sputtering [8]. Tsai *et al.* realized the increase of the PCE of MoS_2/Si from 4.64% to 5.23% in Al/Si solar cells [9]. Rimjhim Chandhary achieved the efficiency up to 12.44% in MoS_2/Si heterojunction solar cell through simulation [10]. Comparatively speaking, the performances of solar cell in experimental results are poorer than the simulation results. This is because solar cell in experiment is affected by some uncontrollable factors and not optimized, which make the solar cell not in optimal conditions. While the previous works are focused on the fabrication of MoS_2/c-Si heterojunction, little understanding of device physics is obtained. In order to improve the efficiency of solar cell, especially effect and physics mechanism of device structure parameters has been concerned such as the intrinsic layer, the defect in MoS_2/Si interface, the BSF, the thickness of MoS_2 etc.

As is well known, the heterojunction with intrinsic thin layer (HIT) solar cell is the best module in Si-based cells with the highest efficiency up to now. It can be expected that the MoS_2/Si heterojunction, combined with HIT, would become one of good ways to develop high-performance solar cells. In this paper, detailed studies of the property of MoS_2/c-Si have been carried out with AFORS-HET. In order to deeply understand the physics of this device, we analyzed the influence of intrinsic layer on performance of TCO/n-type MoS_2/i-layer/p-type c-Si/Al cells, and studied the relationships between the cell parameters, such as thickness and band gap of intrinsic layer, thickness of MoS_2, density of defect states (DOS) and the energy band offset of MoS_2/c-Si interface, and characteristics of heterojunction cells, to improve the performance of solar cell. By optimization of the various cell parameters, we obtained the optimal solar cell structure of TCO/n-type MoS_2/i-type nc-Si:H/p-type c-Si/BSF/Al solar cell with efficiency of 27.22%.

2. Physical Model and Device Structure

2.1. Physical Model

AFORS-HET is used to analyse and simulate the properties of heterojunction solar cells by solving the one-dimensional semiconductor equation based on

Shockley-Read-Hall recombination statistics. In the simulation mode, the energy band electron distributions of solar cells include the valence band, the conduction band extension state, the localized states of valence band tail and the localized states of interval domain. The localized states in the band gap are mainly caused by the dangling bond. The tail domain is mainly caused by strain bond angle. The localized states in the band gap have a double Gaussian function distribution, which were positively correlated. Its distribution equations as follows

$$g_A(E) = G_{AG} \exp\left\{-1/2\left[\left(E - E_{pka}\right)^2 / \sigma_A^2\right]\right\} \quad (1)$$

$$g_D(E) = G_{DG} \exp\left\{-1/2\left[\left(E - E_{pkd}\right)^2 / \sigma_D^2\right]\right\} \quad (2)$$

where E_{pka} and E_{pkd} are the Gaussian peak positions of the acceptor and donor states; σ_A and σ_D are the full width at half maximum (FWHM) of the acceptor and donor states, respectively; G_{AG} and G_{DG} are the density of the acceptor state and the density of the donor state.

Density of location state in band tail is described by an exponential function, and its distribution in the forbidden band are shown in equations (3) and (4) respectively.

$$g_A(E) = G_{A0} \exp\left[\left(E - E_c\right)/E_A\right] \quad (3)$$

$$g_D(E) = G_{D0} \exp\left[\left(E_V - E\right)/E_D\right] \quad (4)$$

where g_A (E) is conduction band tail defect density of states; g_D (E) is valance band tail defect density of states. E_C is conduction band edge; E_V is the valance band edge. G_{A0} and G_{D0} are prefactor; E_A and E_D indicate tail characteristics of the energy transfer. These complex states take the role of traps and composite centers. The composite model mainly considers SRH and Auger recombination, which have a decisive influence on the electrical and optical properties of thin film silicon materials.

2.2. Device Structure

Sanyo Ltd. has developed a silicon heterojubction solar cell named heterojunction with intrinsic thin layer with an efficiency up to 20%, which makes the HIT structure popular. However continuing to improve the efficiency of HIT solar cell is a big challenge. Owing to the unique electronic characteristics and stronger photoresponsivity in visible light spectrum from 400 nm to 680 nm [11] than Siand GaAs, the monolayer MoS_2 was used as window layer to make up a novel HIT cell. The intrinsic layer and back surface field (BSF) layer adopted to improve the efficiency of solar cell. Transparent conductive film (TCO) and Al back contact are also considered. The structure of solar cell is shown in **Figure 1**. The main parameters we draft are shown in **Table 1**, which are taken from various references [10] [12] [13] [14] [15]. For the c-Si, defect density is chosen as oxygen defect at 0.55 eV with a concentration of 1×10^{11} cm^{-3}. The surface re-

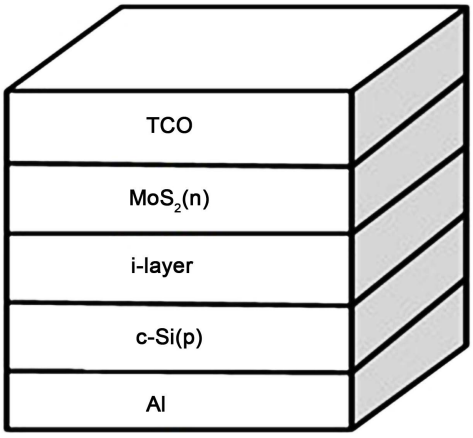

Figure 1. Device structure.

Table 1. Parameters used in present simulation.

Parameter	c-Si (p)	MoS_2	nc-Si: H (i)	a-Si: H (i)	a-SiGe: H (i)	μc-Si (P+)
Thickness (μm)	300	6.5×10^{-4}	4×10^{-3}	4×10^{-3}	4×10^{-3}	1×10^{-2}
Dielectric constant (eV)	11.9	11.9	11.9	11.9	11.9	11.9
Electron affinity (eV)	4.05	4	3.8	3.8	3.9	4
Bandgap (eV)	1.124	1.8	variable	1.74	1.4	1.45
Effective conduction band density (cm^{-3})	2.8×10^{19}	1×10^{19}	1×10^{20}	1×10^{20}	1×10^{20}	1×10^{19}
Effective valence band density (cm^{-3})	1.1×10^{19}	9×10^{20}	1×10^{20}	1×10^{20}	1×10^{20}	1×10^{19}
Electron mobility ($cm^2 \cdot V^{-1} \cdot s^{-1}$)	1×10^{7}	200	20	20	20	50
Hole mobility ($cm^2 \cdot V^{-1} \cdot s^{-1}$)	424.6	67	2	5	5	5
Acceptorconcentration (cm^{-3})	1×10^{16}	0	0	0	0	5×10^{21}
Donor concentration (cm^{-3})	0	1×10^{19}	0	0	0	0
Thermal velocity of electrons (cm/s)	1×10^{7}	1×10^{7}	1×10^{7}	1×10^{7}	1×10^{7}	1×10^{7}
Thermal velocity of holes (cm/s)	1×10^{7}	1×10^{7}	1×10^{7}	1×10^{7}	1×10^{7}	1×10^{7}
Band tail density of states ($cm^{-3} \cdot eV^{-1}$)	1×10^{6}	1×10^{19}	2×10^{21}	2×10^{21}	1×10^{21}	1×10^{21}
Characteristic energy (eV) for donors, acceptors		0.04 0.04	0.045 0.035	0.045 0.02	0.03 0.04	0.1 0.07
Capture cross-section for donor states, e, h (cm^2)	1.0×10^{-15} 1.0×10^{-17}	1.0×10^{-15}, 1.0×10^{-17}	1.0×10^{-15} 1.0×10^{-17}	1.0×10^{-15} 1.0×10^{-17}	1.0×10^{-15} 1.0×10^{-17}	1.0×10^{-15} 1.0×10^{-17}
Capture cross-section for acceptor states, e, h (cm^2)	1.0×10^{-17} 1.0×10^{-15}	1.0×10^{-17} 1.0×10^{-15}	1.0×10^{-17} 1.0×10^{-15}	1.0×10^{-17} 1.0×10^{-15}	1.0×10^{-17} 1.0×10^{-15}	1.0×10^{-17} 1.0×10^{-15}
Gaussian density of states (cm^{-3})		1×10^{19}	1×10^{19}	1×10^{18}	1×10^{16}	1×10^{20}
Gaussian peak energy (eV) for donors, acceptors		1.2 1.46	1.12 1.025	0.725 1.025	0.65 0.55	1.16 1.36
Standard deviation (eV)		0.1	0.1	0.1	0.1	0.2
Capture cross-section for donor states, e, h (cm^2)	1.0×10^{-14} 1.0×10^{-15}	1.0×10^{-14} 1.0×10^{-15}	1.0×10^{-14} 1.0×10^{-15}	1.0×10^{-14} 1.0×10^{-15}	1.0×10^{-14} 1.0×10^{-15}	1.0×10^{-14} 1.0×10^{-15}
Capture cross-section for acceptor states, e, h (cm^2)	1.0×10^{-15} 1.0×10^{-14}	1.0×10^{-15} 1.0×10^{-14}	1.0×10^{-15} 1.0×10^{-14}	1.0×10^{-15} 1.0×10^{-14}	1.0×10^{-15} 1.0×10^{-14}	1.0×10^{-15} 1.0×10^{-14}

flectance of the solar cell is 0.1, the backside emissivity is 1. The surface recombination rate of the electrons and holes at the front and rear contact surfaces is 1 × 10^7 cm/s, these coefficients are given in the AFORS-HET software.

3. Results and Discussions

3.1. The Effect of Different Intrinsic Layer on the Performance of TCO/n-Type MoS_2/i-Layer/p-Type c-Si/Al HIT Solar Cell

MoS_2 has layered structure, while crystal Si is a diamond-like structure, hence, when MoS_2 film was deposited straight on the Si surface, this would results in large quantities of lattice defects at the interface [16]. So it is necessary to conduct interface modification before deposited MoS_2 on Si [16]. The buffer layer can balance carrier injection and reduce the leakage current. When intrinsic layer is inserted into MoS_2/c-Si interface, the intrinsic instead of the Si surface forms a contact with MoS_2 film. It is good way for MoS_2/Si solar cell to obtain high performance by introducing the intrinsic layer for solar cell. Therefore, in this paper, we compared the performance of TCO/n-type MoS_2/i-layer/p-type c-Si/Al solar cells by using different intrinsic layer, including a-Si: H, nc-Si:H and a-SiGe:H. The results are listed in Table 2.

According to Table 2, it is clear that the cell with a-SiGe:H as intrinsic layer has the best performances with efficiency 21.85%. However, using the a-Si:H as intrinsic layer of cell has the poor performances, which efficiency just is 13.4%. This result is mainly ascribed to the recombination rate in p/i interface.

In order to explain the results, we investigated the energy band and recombination rate of solar cells. Figure 2(a) and Figure 2(b) are the energy band and the recombination rate of the heterojunction solar cells with different intrinsic layer respectively. As well known, band offset can be observed at interface when two semiconductors with different band gap contact. Therefore, there is different band offset for p region of solar cell with different intrinsic layer. Band offset has

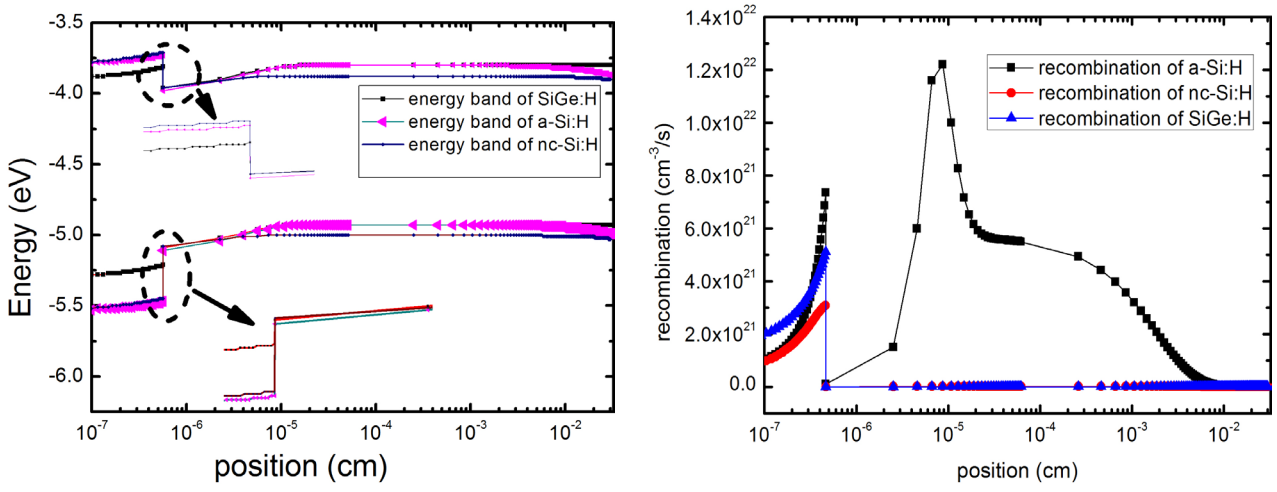

Figure 2. (a)energy band of MoS_2/c-Si cell; (b)recombination rate of MoS_2/c-Si cell.

Table 2. The simulated performance of the solar cells with different intrinsic layer.

Structure of cells	V_{oc} (mV)	J_{sc} (mA/cm^2)	FF	η
TCO/MoS_2/a-Si:H/p-Si/Al	559.5	29.87	80.14	13.4%
TCO/MoS_2/nc-Si:H/p-Si/Al	652.7	39.97	83.7	21.83%
TCO/MoS_2/SiGe:H/p-Si/Al	652.7	40.01	83.7	21.85%

an important impact on the performance of solar cell. According to the Equation (5) [17]

$$J = J_{sc} - \left[\left(qD_n N_d / L_n \right) \exp\left(-\left(qV_D + \Delta E_c \right) / k_0 T \right) + \left(qD_p N_A / L_P \right) \exp\left(-\left(qV_D - \Delta E_V \right) / k_0 T \right) \right] \times \left(\exp\left(qv / k_0 T \right) - 1 \right) \quad (5)$$

It can be noted that when ΔE_V increases, J will be reduced; this will lead to the decreasing of cell performance. From **Figure 2(a)**, when a-Si: H serving as the intrinsic layer, ΔE_V is larger, according to Equation (5) that will result in J smaller and makes the cell efficiency worse. In addition, From **Figure 2(b)**, it shows that the recombination rate of solar cell with a-Si:H as the intrinsic layer is higher, consequently, the recombination rate of the i/p interface is increased, and resulting in the open circuit voltage has a low value, so using a-Si:H as the intrinsic layer of heterojunction solar cell, the efficiency is lower than the other materials. For a-SiGe:H, ΔE_V is small so that the efficiency of the TCO/n-type MoS_2/i-layer/p-type c-Si/Al solar cells with a-SiGe:H as intrinsic layer is higher, reaching 21.85%. For the solar cell with nc-Si:H as the intrinsic layer, it can be seen from **Figure 2(a)** that the conduction band offset is large that equals to 0.25 eV. Conduction band offset suppresses the surface recombination and makes the cell efficiency up to 21.83%.

3.2. Effect of Defect States and the Energy Band Offset of MoS_2/c-Si Interface of the TCO/n-Type MoS_2/i-Layer nc-Si:H/p-Type c-Si/Al HIT Solar Cell

For MoS_2/c-Si heterojunction solar cells, the density of defect states of MoS_2/c-Si interface is the important influencing factor that determines the transport properties of the cell. Here, in this paper, the TCO/n-type MoS_2/i-type nc-Si:H/p-type c-Si solar cell is studied. Because the bandgap adjusted of a-Si: H is less convenient than nc-Si:H. The bandgap of a-SiGe:H is small, though its bandgap is adjustable. Hence, we select the nc-Si:H as intrinsic layer in TCO/n-type MoS_2/i-type/p-type c-Si solar cell. The performances of the solar cell with TCO/n-type MoS_2/i-layer nc-Si:H/p-type c-Si/Al structure as a function of MoS_2/c-Si interface defect states show in **Figure 3**.

From **Figures 3(a)-(d)**, we can see that the larger density of defect state of MoS_2/c-Si interface leads to the decreasing of V_{oc}, J_{sc}, FF and Eff. Initially V_{oc} and J_{sc} slightly decrease with the increasing density of defect state of MoS_2/c-Si interface. However, V_{oc} and J_{sc} obviously decrease when value larger than 1×10^{11} cm^{-2}·eV^{-1}. FF and E_{ff} almost keep at constant initially with increasing density of

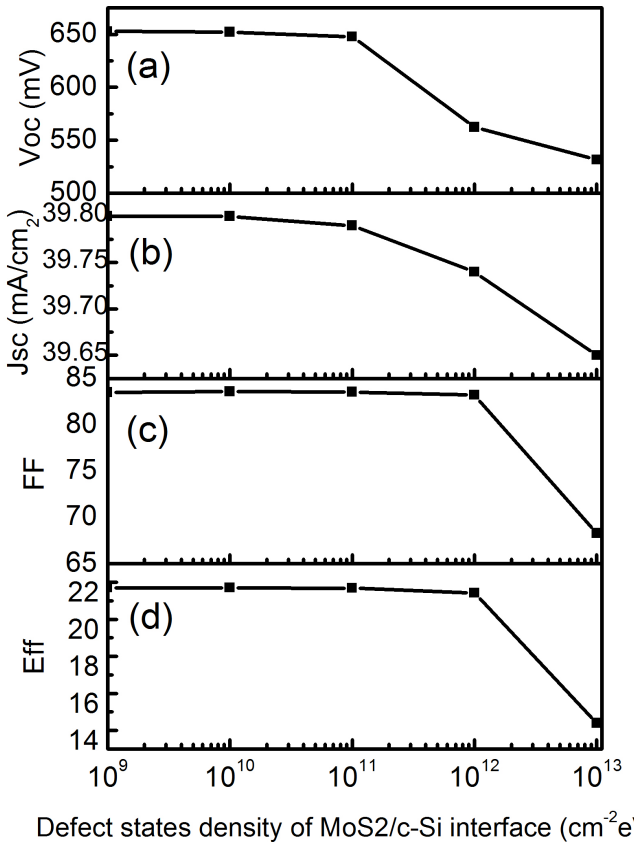

Figure 3. Performances of TCO/n-type MoS_2/i-layer nc-Si:H/p-type c-Si/Al MoS_2/i-layer nc-Si:H/p-type c-Si/Al as a function of defect states. as a function of different ΔE_V.

defect state of MoS_2/c-Si interface, but greater than 1×10^{12} $cm^{-2}{\cdot}eV^{-1}$, they visibly reduce. The results indicate that the density of defect states of interface is less than 1×10^{11} $cm^{-2}{\cdot}eV^{-1}$, the performances of solar cell decrease slowly, however, the performances of solar cell reduce rapidly when the defect states of MoS_2/c-Si interface higher than 1×10^{11} $cm^{-2}{\cdot}eV^{-1}$. Therefore, the density of defect states of interface should be under1×10^{11} $cm^{-2}{\cdot}eV^{-1}$ in order to obtain good performance, and the better performances can be obtained due to the larger J_{sc} when the density of interface defect states is lower than 1×10^{11} $cm^{-2}{\cdot}eV^{-1}$. It is because that defect states of interface and monolayer MoS_2 works as charge carriers traps that provide the channel for carriers recombination.

The photo-generated carriers come mainly from p-type c-Si layer in n-type MoS_2/p-type c-Si heterojunction solar cells. And there is a potential barrier resulting from the valence band offset at n-type MoS_2/p-type c-Si interface, which hinders the photo-generated minority carrier holes from being collected by front electrode. As a result, the valence band offset strongly affects the interface transport properties of photogenerated holes. As well known, the influence of ΔE_V on the interface transport properties and performances of solar cells can be got by changing the electron affinity of n type MoS_2layer and p-type c-Si layer [10]. The performances of TCO/n-type MoS_2/i-layer nc-Si:H/p-type c-Si/Al solar cell as a function of ΔE_V are given in **Figure 4**.

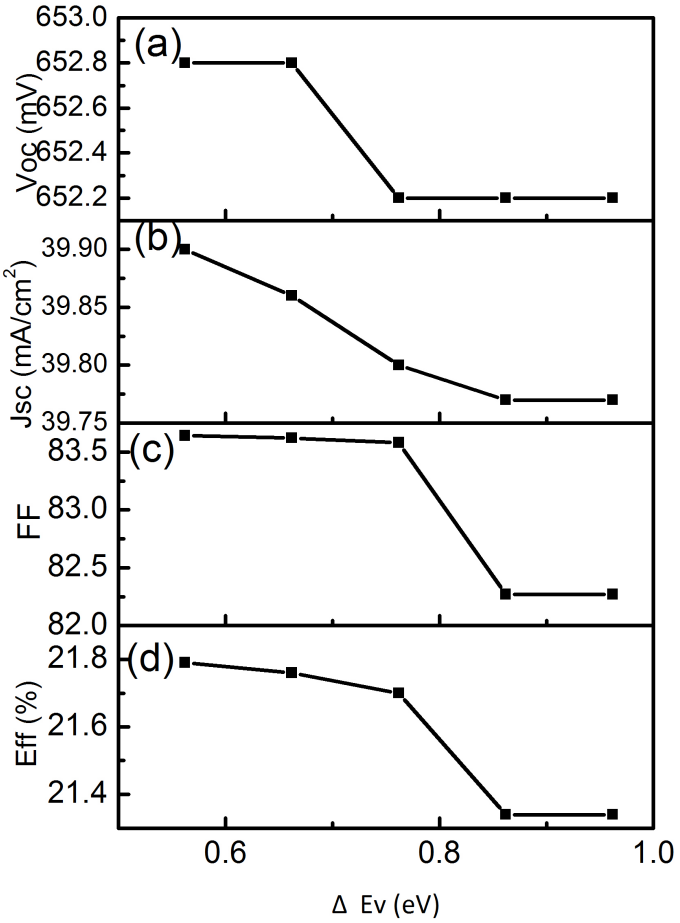

Figure 4. Performances of TCO/n-type TCO/n-type MoS_2/i-layer nc-Si:H/p-type c-Si/Al MoS_2/i-layer nc-Si:H/p-type c-Si/Al as a function of defect states. as a function of different ΔE_V.

As we can see from **Figure 4(a)**, initially the V_{oc} keeps at constant with the increasing of ΔE_V from 0.55 eV to 0.7 eV, then decreases when ΔE_V larger than 0.7 eV, however, when ΔE_V greater than 0.76 eV the value of V_{oc} keeps at constant again. From **Figure 4(b)**, the J_{sc} almost remains at a constant with increasing of ΔE_V. In case of the fill factor, it slightly reduces from 83.64% to 83.58% with increasing of ΔE_V from 0.56 eV to 0.76 eV. However, the value keeps at constant when ΔE_V greater than 0.86 eV. E_{ff} decreases continuously with the increasing of ΔE_V. It is found that when ΔE_V is under 0.762 eV, ΔE_V has little impact on J_{sc} and FF, with the increasing of ΔE_V, J_{sc} stands at fixed value, but FF and V_{oc} decrease. It indicates that an appropriate high minority carrier band offset can lead to an effective suppression of interface recombination at MoS_2/c-Si hetero-interface, but too high band offset may enhance the interface recombination. So it is evident that ΔE_V should be kept lower than 0.762 eV in order to obtain good performance of solar cell. For this result, we studied the energy band structure with different ΔE_V, the results display in **Figure 5**.

As we can see form **Figure 5**, the degree of band bending at interface between MoS_2 and c-Si increases when ΔE_V is larger, which will lead to the higher valence

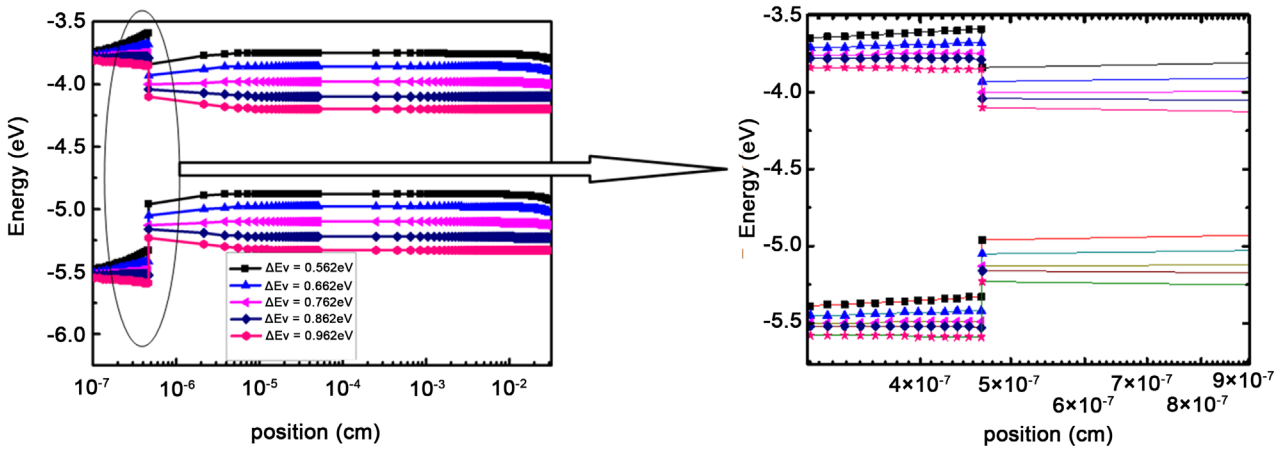

Figure 5. The energy band structure of the cell with different ΔE_V.

band barrier for holes and enhancing the build-in potential. From Equation (5), it is easy to note that J will decrease with the increasing of ΔE_V, and then the performance of the solar cell will go bad. The offsets between the band edges, ΔE_C and ΔE_V of the MoS_2/c-Si junction influence strongly the carrier transporting across the hetero-interface, so setting the suitable carrier band offset is necessary. Above all, the defect state of MoS_2/c-Si interface should be under 1×10^{11} $cm^{-2}\cdot eV^{-1}$, and the ΔE_V should be under 0.762 eV so that we can get the good performance for solar cell. It implies that the monolayer MoS_2 is a potential material for solar cell if we deal well the MoS_2/c-Si interface.

3.3. Optimizing the Performance of TCO/n-Type MoS_2/i-Layer nc-Si:H/p-Type c-Si/Al Heterojunction Solar Cells with BSF

It is known that BSF working as passivation plays an important role in improving the performance of solar cell [18]. In order to improve the performances of solar cell, the effect of BSF on the performance of the cell was studied by TCO/n-type MoS_2/i-typenc-Si:H/p-type c-Si/BSF/Al cell structure in this paper. We choose p + -μc-Si:H as back surface layer. On one hand, the band gap of p + -a-Si:H is about 1.74 eV, and it has a large ΔE_c because of its large band gap which has a good effect on the reflection of electrons. On the other hand, nevertheless, ΔE_V also increases resulting in the holes difficultly reach to the back electrode. Compared with p + -a-Si:H, the bandgap of p + -μc-Si:H is about 1.45 eV, that is to say, the ΔE_c is relatively low which can lessen the reflection of the effective electrons. Furthermore, the electrons of the back surface field are collected, therefore, using p + -μc-Si:H as the back surface layer can transport enough of the majority of carriers [18]. The optimizing result is shown in **Figure 6**.

Figure 6 is the J-V curve of TCO/n-typeMoS_2/i-layer nc-Si:H/p-type c-Si/BSF/Al solar cells. According to **Figure 6**, the result reveals that the open circuit voltage of solar cell increases from 652.7 mV to 771.1 mV, in case of short-circuit current density, it increases from 39.97 mA/cm^2 to 42.46 mA/cm^2 and cell efficiency increases from 21.83% to 26.99%. It is obvious that the

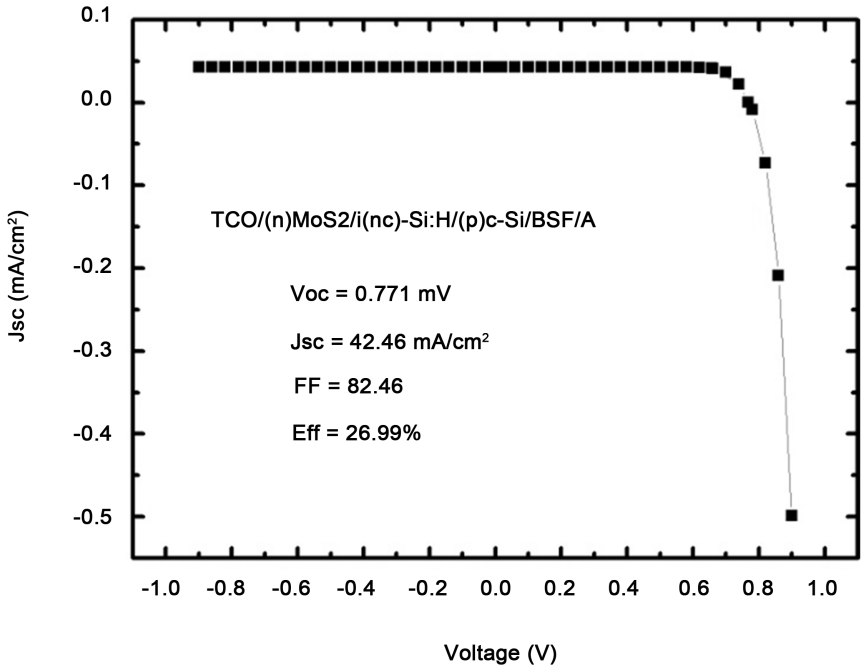

Figure 6. J-V curve of TCO/n-type MoS_2/i-typenc-Si: H/p-type c-Si/BSF/Al solar cell.

performances of the solar cell with BSF are obviously improved. It means that BSF is a good way to improve the performance of solar cell. BSF can collect the photogenic minority carrier in back surface, improving the internal quantum efficiency of solar cell. In addition, BSF layer can introduce barrier for minority carriers, which can reduce the recombination of the photons on the surface.

3.4. Effects of nc-Si:H Intrinsic Layer on the Performance of Solar Cell

3.4.1. The Optimization of Band Gap of nc-Si:H Intrinsic Layer

The intrinsic layer plays an important role in interfacial modification and band offset of solar cell, consequently, optimizing the intrinsic band gap to improve the efficiency of solar cells is necessary. Therefore, in this section, the band gap of intrinsic layer is variable from 1.6 eV to 1.8 eV, other parameters keep at constant.

The performances curve of the solar cell with different band gap of nc-Si: H is presented in **Figure 7**. According to **Figure 7(a)**, the open-circuit voltage V_{oc} increases obviously from 766.6 mV to 771.6 mV with the increase of intrinsic band gap from 1.60 eV to 1.80 eV. From **Figure 7(b)**, increasing with the energy gap, the J_{sc} almost holds at constant, it means that the band gap of the intrinsic layer has little effect on the short-circuit current density. **Figure 7(c)** indicates that the FF decrease obviously from 82.82% to 82.41%. In case of E_{ff}, it is found that the E_{ff} keeps at constant nearly with the increases of intrinsic band gap. The observably improvement of the open voltage is attributed to the change of barrier in the MoS_2/c-Si solar cell, causing the smaller probability of carrier at the interface in the heterojunction smaller, thus the reverse saturation current

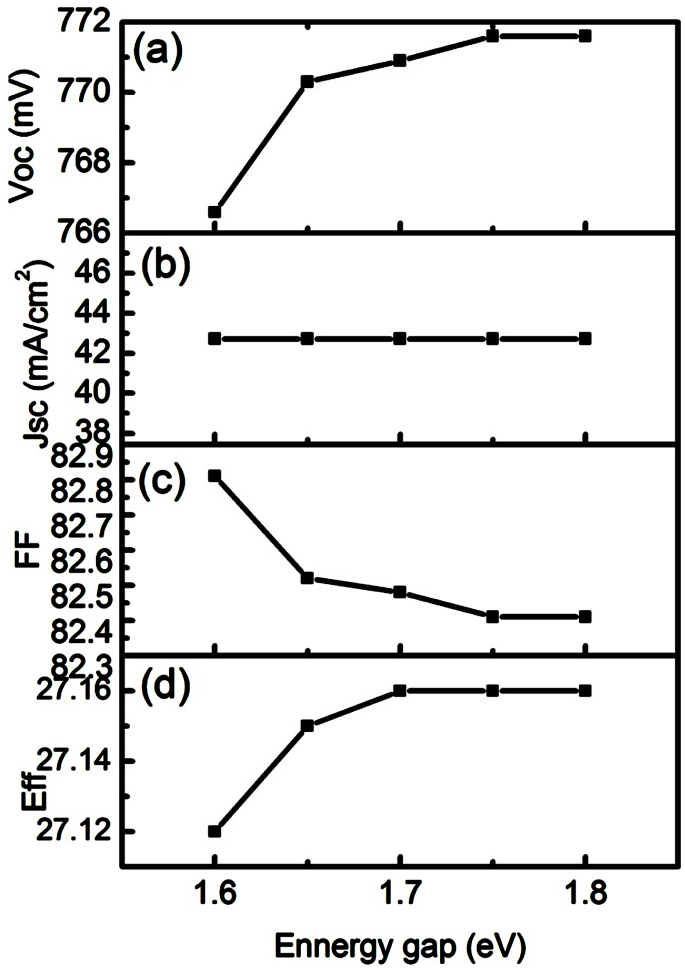

Figure 7. Performances of TCO/n-type MoS_2/i-type nc-Si:H/p-type c-Si/BSF/Al with different band gap of intrinsic layer.

decreases in p-n junction, but the open circuit voltage increases. The FF decreases with the increase of band gap due to the increase in the open-circuit voltage V_{oc}. The conversion efficiency of the cell slowly enhances with the increase of the band gap. The efficiency is basically kept constant when the band gap become more than 1.7 eV. Hence, the intrinsic band gap of 1.7 eV was optimized for achieving high performance of cell which efficiency up to 27.16%.

3.4.2. Optimization of the Thickness of nc-Si: H Intrinsic Layer

Figures 8(a)-(d) show the performances curves of TCO/n-type MoS_2/i-layer nc-Si:H/p-type c-Si/BSF/Al solar cells with different thickness. From **Figure 8(a)**, it can be noted that the open circuit voltage Voc decreases gradually from 771.6 mV to 762.8 mV with the thickness increases from 2 nm to 10 nm, **Figure 8(b)** displays that the short current density continuously reduces from 42.81 mA/cm^2 to 42.16 mA/cm^2 with increases of thickness. **Figure 8(c)** indicates that the FF initially increases slightly with the increase of the intrinsic layer thickness from 2 nm to 8 nm. However, when thickness of nc-Si:H greater than 8 nm, the FF gradually decreases. It is depicted in **Figure 8(d)**, with the thickness of the

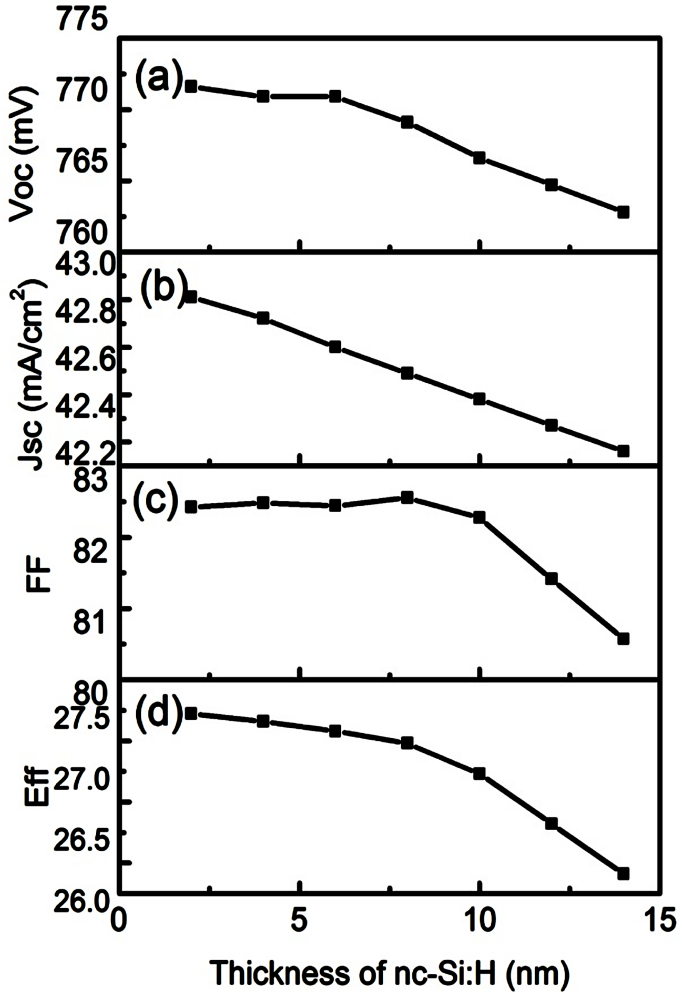

Figure 8. Performances of TCO/n-type MoS_2/i-type nc-Si:H/p-type c-Si/BSF/Al with different thickness of intrinsic layer.

intrinsic layer is variable from 2 nm to 14 nm, the efficiency of the cell is reduced rapidly from 27.16% to 25.91%. The decrease of the open voltage can be attributed to an decrease of the built-in electric field. The quantum efficiency characteristic of the cells with different thicknesses of intrinsic layer is used to explain these results, as shown in Figure 9.

Figure 9 shows the quantum efficiency characteristic of the cells with various values of thickness of intrinsic layer. It is obvious that the short-wave response of the cell is deteriorated with the increase of the thickness of nc-Si:H. According to the Equation (6) and Equation (7), this will lead to the photogenerated current and the open circuit voltage decrease. It indicates that the corresponding photogenerated carriers are not collected effectively, which leads to a decrease in Jsc of the cell.

$$J_{sc} = q\int \varphi(\lambda)\{1-R(\lambda)\}QE(\lambda)\mathrm{d}\lambda \tag{6}$$

$$V_{oc} = (nkT/q)\ln(1+J_{ph}/J_0) \tag{7}$$

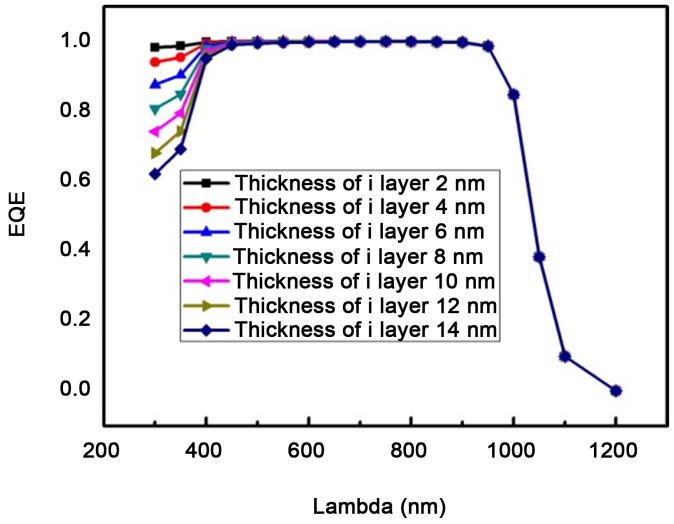

Figure 9. The QE curve of solar cell with different thickness.

Since E_{ff} varies in proportion with V_{oc} and J_{sc}, therefore, efficiency of solar cell will reduce with the photogenerated current and the open circuit voltage decreasing.

3.5. Optimization of Thickness of n-Type MoS_2 Emitter Layer

Figures 10(a)-(d) show the cell performance of solar cells with the different MoS2 thickness. From **Figure 10(a)**, it is evident that Voc indicates that the thickness of MoS_2 has no effect on Voc. However, **Figure 10(b)** shows that the short-circuit current density decreases gradually from 42.49 mA/cm^2 to 42.16 mA/cm^2 with the increasing MoS_2 thickness from 0.65 nm to 9.75 nm. For **Figure 10(c)**, we can see that the value of fill factor follows oscillating behaviour with increasing the thickness of MoS_2 but it continuously reduces from 82.49% to 82.43% in the thickness range 1.95 to 7.15 nm, and it reaches a maximum of 82.49% for the thickness at 8.45 nm. From **Figure 10(d)**, we can note that the efficiency of solar cell decreases from 27.22% to 26.8% with increasing the thickness of MoS_2. The reduction of Jsc may be ascribed to the increase in absorption losses at the surface layer and the larger series resistance in solar cell. The monolayer MoS_2 is a direct gap which is beneficial to electron jumping. Hence, we can achieve the best performance of the cell up to 27.22% at the thickness of MoS_2 is 0.65 nm. But the efficiency reduces with increasing the thickness of MoS_2 due to it is indirect gap for multilayer MoS_2.

3.6. Optimization the Best Performance of MoS2/c-Si Solar Cell

From the above work we did, we finally obtained the best performance of solar cell which efficiency is up to 27.22% with the density of defect states and band offset of MoS_2/c-Si interface lower than 1×10^{11} cm^{-2}·eV^{-1} and 0.762 eV respectively, MoS_2 thickness of 0.65 nm, intrinsic layer thickness of 2 nm and the band gap is 1.7 eV. The J-V curve of solar cell is shown in **Figure 11**.

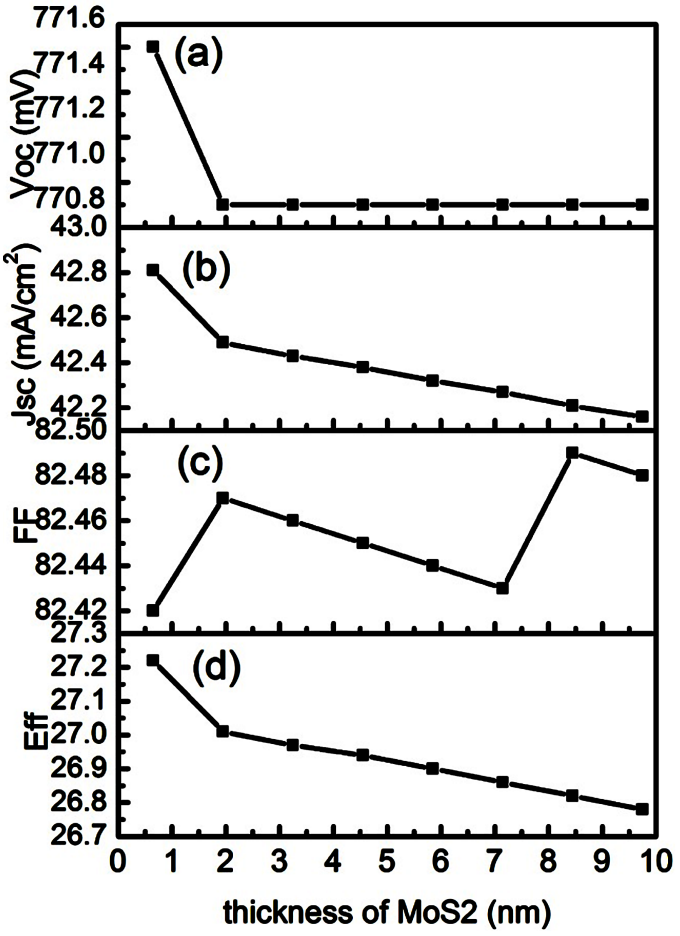

Figure 10. Performances of TCO/n-type MoS_2/i-type nc-Si:H/p-type c-Si/BSF/Al with different thickness of MoS_2.

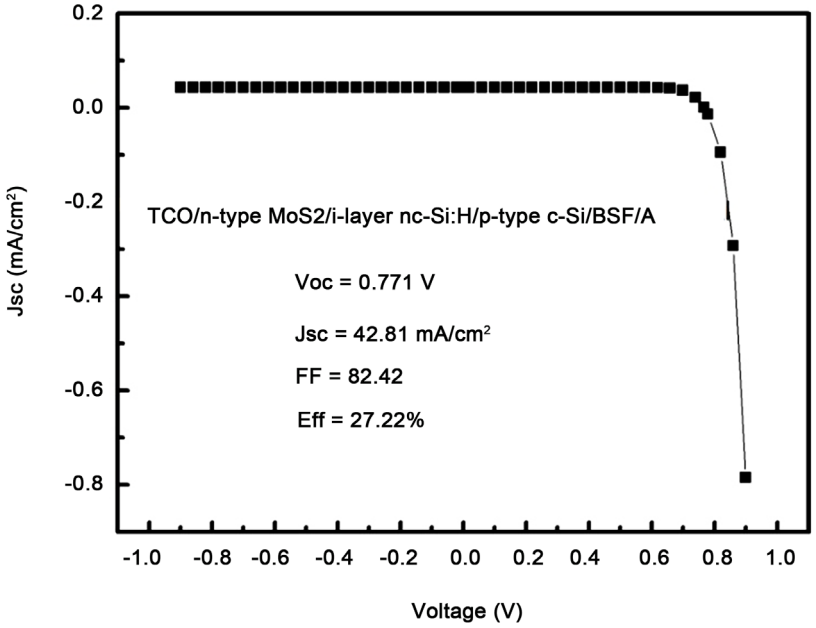

Figure 11. J-V curve of solar cell with best performance.

4. Conclusions

The TCO/n-type MoS_2/i-layer nc-Si:H/p-type c-Si/Al solar cells were investigated by AFORS-HET. The main studies are the intrinsic layer selection and optimization, MoS_2/c-Si interface optimization and the effect of BSF layer on the cell performance. The effect of different intrinsic layers including a-Si:H, nc-Si:H and a-SiGe:H on solar cells was studied. For intrinsic layer a-SiGe:H, the solar cell has the best performance with the efficiency 21.85%. The results show that when the density of defect states is lower than 1×10^{11} $cm^{-2} \cdot eV^{-1}$ and the band offset is lower than 0.762 eV, the solar cell has better performances. The parameters of optimal cell structure with TCO/n-type MoS_2/i-layer nc-Si:H/p-type c-Si/BSF/Al are, thickness of MoS_2 0.65 nm, intrinsic layer thickness of 2 nm and the band gap of 1.7 eV, with the open circuit voltage V_{oc} 771.6 mV, J_{sc} 42.81 mA/cm^2, fill factor FF 82.42%, conversion efficiency of cell up to 27.22%.

Acknowledgements

This work is supported by the National Natural Science Foundation of China (Grant No. 51472096), the R & D Program of Ministry of Education of China (No. 62501040202). The authors would like to acknowledge Helmholts-Zentrum Berlin for providing AFORS-HET simulation software.

References

[1] Pham, T.A., Choi, B.C. and Jeong, Y.T. (2010) Facile Covalent Immobilization of Cadmium Sulfide Quantum Dots on Graphene Oxide Nanosheets: Preparation, Characterization, and Optical Properties. *Nanotechnology*, **21**, Article ID: 465603. https://doi.org/10.1088/0957-4484/21/46/465603

[2] Addou, R., Colombo, L. and Wallace, R.M. (2015) Surface Defects on Natural MoS_2. *ACS Applied Materials & Interfaces*, **7**, 11921-11929. https://doi.org/10.1021/acsami.5b01778

[3] Li, X. and Zhu, H. (2015) Two-Dimensional MoS_2: Properties, Preparation, and Applications. *Journal of Materiomics*, **1**, 33-44. https://doi.org/10.1016/j.jmat.2015.03.003

[4] Ganatra, R. and Zhang, Q. (2014) Few-Layer MoS_2: A Promising Layered Semiconductor. *ACS Nano*, **8**, 4074-4099. https://doi.org/10.1021/nn405938z

[5] Nishiguchi, K., Castellanos-Gomez, A., Yamaguchi, H., *et al.* (2015) Observing the Semiconducting Band-Gap Alignment of MoS_2 Layers of Different Atomic Thicknesses Using a MoS_2/SiO_2/Si Heterojunction Tunnel Diode. *Applied Physics Letters*, **107**, Article ID: 053101. https://doi.org/10.1063/1.4927529

[6] Tao, J., Chai, J., Lu, X., *et al.* (2015) Growth of Wafer-Scale MoS_2 Monolayer by Magnetron Sputtering. *Nanoscale*, **7**, 2497-2503. https://doi.org/10.1039/C4NR06411A

[7] Bernardi, M., Palummo, M. and Grossman, J.C. (2013) Extraordinary Sunlight Absorption and One Nanometer Thick Photovoltaics Using Two-Dimensional Monolayer Materials. *Nano Letters*, **13**, 3664-3670. https://doi.org/10.1021/nl401544y

[8] Hao, L., Liu, Y., Gao, W., *et al.* (2015) Electrical and Photovoltaic Characteristics of MoS_2/Sip-n Junctions. *Journal of Applied Physics*, **117**, Article ID: 114502. https://doi.org/10.1063/1.4915951

[9] Tsai, M., Su, S., Chang, J., *et al.* (2014) Monolayer MoS_2 Heterojunction Solar Cells. *ACS Nano*, **8**, 8317-8322. https://doi.org/10.1021/nn502776h

[10] Chaudhary, R., Patel, K., Sinha, R.K., *et al.* (2016) Potential Application of Mono/Bi-Layer Molybdenum Disulfide (MoS_2) Sheet as an Efficient Transparent Conducting Electrode in Silicon Heterojunction Solar Cells. *Journal of Applied Physics*, **120**, Article ID: 013104. https://doi.org/10.1063/1.4955071

[11] Lopez-Sanchez, O., Lembke, D., Kayci, M., *et al.* (2013) Ultrasensitive Photodetectors Based on Monolayer MoS_2. *Nature Nanotechnology*, **8**, 497-501. https://doi.org/10.1038/nnano.2013.100

[12] Rawat, A., Sharma, M., Chaudhary, D., *et al.* (2014) Numerical Simulations for High Efficiency HIT Solar Cells using Microcrystalline Silicon as Emitter and Back Surface Field (BSF) Layers. *Solar Energy*, **110**, 691-703.

[13] Zhao, L., Wang, G., Diao, H., *et al.* (2016) Theoretical Investigation on the Passivation Layer with Linearly Graded Bandgap for the Amorphous/Crystalline Silicon Heterojunction Solar Cell. *Rapid Research Letters*, **10**, 730-734.

[14] Zhao, L., Zhou, C.L., Li, H.L., *et al.* (2008) Design Optimization of Bifacial HIT Solar Cells on P-Type Silicon Substrates by Simulation. *Solar Energy Materials and Solar Cells*, **92**, 673-681.

[15] Zeng, X.B., Xian, Yi.X.,Wen, X.X. and Liao, W.G. (2014) Analysis of the Optimization Design for nc-Si/c-Si Heterojunction Structure Solar Cells. *Acta Energiae Solaris Sinica*, No. 9, 561-1567.

[16] Hao, L.Z., Gao, W., Liu, Y.J., *et al.* (2015) High-Performance n-MoS_2/i-SiO_2/p-Si Heterojunction Solar Cells. *Nanoscale*, **7**, 8304-8308. https://doi.org/10.1039/C5NR01275A

[17] Wen, X., Zeng, X., Liao, W., *et al.* (2013) An Approach for Improving the Carriers Transport Properties of a-Si:H/c-Si Heterojunction Solar Cells with Efficiency of more than 27%. *Solar Energy*, **96**, 168-176.

[18] Dao, V.A., Heo, J., Choi, H., *et al.* (2010) Simulation and Study of the Influence of the Buffer Intrinsic Layer, Back-Surface Field, Densities of Interface Defects, Resistivity of p-Type Silicon Substrate and Transparent Conductive Oxide on Heterojunction with Intrinsic Thin-Layer (HIT) Solar Cell. *Solar Energy*, **84**, 777-783.